

# THE CONTINUOUS ELECTRON BEAM ACCELERATOR FACILITY: CEBAF at the Jefferson Laboratory

---

Christoph W. Leemann, David R. Douglas, and  
Geoffrey A. Krafft

*Thomas Jefferson National Accelerator Facility, Newport News, Virginia 23606;  
e-mail: Leemann@JLab.org, Douglas@JLab.org, Krafft@JLab.org*

**Key Words** superconducting radiofrequency, polarization, recirculating  
accelerator, energy spread, high average current

■ **Abstract** The Jefferson Laboratory's superconducting radiofrequency (srf) Continuous Electron Beam Accelerator Facility (CEBAF) provides multi-GeV continuous-wave (cw) beams for experiments at the nuclear and particle physics interface. CEBAF comprises two antiparallel linacs linked by nine recirculation beam lines for up to five passes. By the early 1990s, accelerator installation was proceeding in parallel with commissioning. By the mid-1990s, CEBAF was providing simultaneous beams at different but correlated energies up to 4 GeV to three experimental halls. By 2000, with srf development having raised the average cavity gradient to 7.5 MV/m, energies up to nearly 6 GeV were routine, at 1–150  $\mu$ A for two halls and 1–100 nA for the other. Also routine are beams of >75% polarization. Physics results have led to new questions about the quark structure of nuclei, and therefore to user demand for a planned 12 GeV upgrade. CEBAF's enabling srf technology is also being applied in other projects.

## CONTENTS

INTRODUCTION .....	414
HISTORICAL PERSPECTIVE AND DEVELOPMENT OF CONCEPT .....	417
Adoption of SRF Technology .....	417
Recirculation and Beam Optics .....	419
Beam Delivery and Operational Aspects .....	420
Beam Polarization .....	421
Accelerator Physics .....	421
Parameter List .....	421
PROJECT ENGINEERING AND CONSTRUCTION .....	422
Machine Overview .....	422

Building Cryomodules (Design and Process) .....	425
Cryogenics System .....	426
RF Systems .....	429
Beam Transport .....	430
Control System .....	432
COMMISSIONING, MACHINE PERFORMANCE, AND SCIENCE .....	433
Polarized Source Development .....	434
Machine Performance .....	436
Physics Results .....	438
Spinoffs and Parallel Efforts .....	439
The Infrared Demonstrator Free-Electron Laser .....	439
SRF Systems for the Spallation Neutron Source .....	440
FUTURE DIRECTIONS .....	440
Basic Design Considerations for Higher Energy .....	441
CEBAF 12 GeV Upgrade .....	442
Comparison with Electron Linac for Europe (ELFE) .....	443
Energy-Recovered Linacs .....	445
CONCLUSIONS .....	446

## INTRODUCTION

Around 1980 a consensus began to form among nuclear physicists that a new kind of electron accelerator was needed for studies at the nuclear and particle science interface: the transition region between the energy regime where strongly interacting matter is understood as nucleon bound states and the regime where the underlying quark-gluon structure appears. This desire was reflected in formal long-range plans issued in 1979 and 1983 by the U.S. Nuclear Science Advisory Committee (NSAC). Chartered jointly by the National Science Foundation and the Department of Energy, this body called for a new national accelerator to meet the identified need. A 1984 NSAC panel characterized the physics desiderata as they were then understood:

[We] assigned highest scientific priority to investigation of hadron structure and two body interactions, three and four body systems, and fundamental symmetries . . . to study the largely unexplored transition between the nucleon-meson and the quark-gluon descriptions of nuclear systems (1).

Ultimately, the construction and mid-1990s initial operation of the Continuous Electron Beam Accelerator Facility (Figure 1) at what came to be called the Thomas Jefferson National Accelerator Facility—CEBAF at the Jefferson Laboratory—resulted (2). For transition-region experiments, the originally envisioned machine required a combination of characteristics: multi-GeV energy for spatial resolution and kinematic flexibility, high intensity for precise measurement of relatively small electromagnetic cross sections, high duty factor to allow coincidence



**Figure 1** Aerial view of the CEBAF accelerator complex. Service building locations indicate the racetrack shape of the underground accelerator, which sends beams to the three domed, partly underground experimental halls in the foreground.

experiments, and beam quality sufficient for use with high-resolution spectrometers and detectors.

Understood from the outset to be essential for the new accelerator were continuous wave (cw) operation, currents up to  $200 \mu\text{A}$ , and simultaneous delivery of beams to multiple users. The importance of beam polarization emerged during construction as the science program became more crisply defined. The beam energy, originally specified as 4 GeV, was a subject of ongoing debate, which encouraged design choices that would not preclude a later energy upgrade. Independent of, but in parallel to, the emergence of these user requirements, development within the accelerator community of superconducting radiofrequency (srf) technology had by 1985 progressed sufficiently to contemplate industrial-scale application (3–8). This

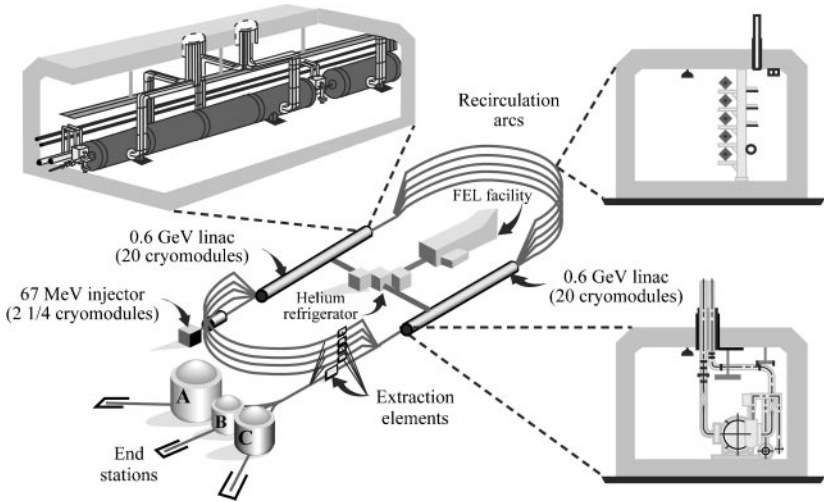


**Figure 2** Schematic CEBAF accelerator overview.

coincidence of physics requirements with the maturing of a novel technology presented a unique opportunity, which allowed the design, construction, and successful operation of an accelerator that has not only exceeded initial user expectations, but in fact readily incorporates evolving user requirements and, moreover, presents immediate prospects for straightforward upgrades to significantly higher energies.

The CEBAF accelerator is a five-pass recirculating srf linac (Figure 2) capable of simultaneous delivery to three end stations of cw beams of up to  $200 \mu\text{A}$  with 75% polarization, geometric emittance less than  $10^{-9}$  m rad, and relative momentum spread of a few  $10^{-5}$ . The lowest operating energy is about 0.6 GeV, the present full energy is nearly 6 GeV, and a cost-effective upgrade to 12 GeV is possible and planned. The combination of five-pass recirculation, a three-laser photocathode source, and subharmonic-rf-separator-based extraction enables simultaneous delivery of three beams at different energies, with hall-to-hall current ratios approaching  $10^6$ , and with a specified orientation of the beam polarization.

The most important innovations in CEBAF are the choice of srf technology and use of multipass beam recirculation. Neither had been previously applied on the scale of CEBAF. In fact, until LEP II came into operation, CEBAF was the world's largest implementation of srf technology, the use of which ensures the possibility of energy upgrades, enabling forefront research for years to come. Beam recirculation minimizes the cost of the srf implementation and has been executed with bend radii large enough to keep open the possibility of future energy upgrades.

## HISTORICAL PERSPECTIVE AND DEVELOPMENT OF CONCEPT

The CEBAF project entailed certain significant changes and developments as it progressed from conceptual design through construction and commissioning and into operation (9–13). These included a transition from conventional (copper-based) accelerating technology to srf technology, utilization of multipass beam recirculation, provision for simultaneous cw beam delivery to multiple experiments, accelerated implementation of polarized source technology, and the resolution of accelerator physics and design issues imposed by these changes. The following overview of these topics places them into a historical context illuminating subsequent technical descriptions of the accelerator.

### Adoption of SRF Technology

The adoption of srf technology was a seminal event, defining CEBAF as implemented today (14). A cw linac is the solution of choice for a simple multi-GeV cw accelerator for high-quality beams. However, a 4 GeV normal conducting linac has an active length of 1 1/3 km, and consumes 240 MW average rf power, assuming a cw accelerating field of 3 MV/m and a typical shunt impedance of 50 M $\Omega$ /m. Therefore, to reduce project cost, proposals prior to 1985—based on normal conducting rf technology—relied on technological alternatives such as multiple recirculation of the beam through the acceleration structure (microtrons) or systems based on pulsed linacs with pulse stretcher rings. Unfortunately, such solutions frequently encountered limitations preventing performance at the levels both desired by users and accessible to the excessively expensive full-energy cw linac.

Microtrons, for example, experience beam current limitations from instabilities driven by the multiple passages of the beam through the acceleration structure. They may, in addition, be limited to modest (few-GeV) final energies by synchrotron-radiation-driven degradation of beam quality during recirculation. Pulsed linacs with pulse stretchers suffer the ills associated with high-power pulsed systems and are subject to tight timing tolerances and operational complexity to produce cw beams of high quality. Neither of these systems presents a simple path for energy upgrades.

CEBAF as originally approved was to be a 2 GeV, S-band, disc-loaded, pulsed, room-temperature linac that would reach 4 GeV by one “head-to-tail” recirculation, and that would provide cw beams to experiments through the use of a pulse stretcher ring (15). This concept had no identifiable hard failure mode. A contract to implement such an accelerator at a capital cost of \$225 million was awarded by the U.S. DOE in 1984 to the Southeastern Universities Research Association (SURA). Concerns arose, however, and several potential shortcomings in the initial design became evident. Conventional technology was pushed to its limits. The high bunch charge would limit the achievable emittance in at least the horizontal

plane, fast (less than 1 ms) resonant extraction was sure to present challenges of its own, and a cost-effective path to higher energies was not evident.

In June 1985, C. Leemann was charged to conduct a systematic evaluation of the applicable technology base. It became apparent that srf technology had made significant progress in the 1970s and early 1980s, far beyond what was common knowledge among the majority of accelerator physicists and engineers. An srf approach would, moreover, provide beam quality well in excess of that available from alternatives and presented a straightforward path for extensions to much higher energies. In September 1985, CEBAF management unanimously decided to request a change from the baseline room-temperature design. After extensive external review, and interim reviews at critical stages of the evolving new design concept, a Conceptual Design Review by the U.S. DOE accepted the change by February 1986 (16). Given a schedule of a few months to design, document, and review what was then the world's largest srf application, a novel or unique cavity design including power and higher-order-mode (HOM) couplers could not be developed. It was instead to be copied from pre-existing paradigms, which included the 350 MHz cavities under development for a first LEP improvement, the 500 MHz cavities developed at DESY and KEK to boost luminosity and energy in PETRA and TRISTAN, the 1500 MHz cavities developed at Cornell University's Newman Laboratory for the upgrade to CESR II (7), and the 3000 MHz cavities developed at the Bergische Universität Wuppertal in Germany for a small linac installation in Darmstadt.

In general terms it was reasonable to expect higher accelerating gradients, but also higher HOM shunt impedances, from higher frequencies. Cryogenic system cost optimization (17) showed that the higher frequencies call for 2 K operating temperature, while for the lower ones about 4 K is acceptable even if not optimal. From the user perspective, frequencies had to be high enough to run with full current while avoiding generation of multiple events by a single beam bunch. On balance, 1500 MHz was a good choice. Ultimately, however, the decisive technical reasons for choosing the Cornell design were the extraordinarily well-developed understanding of HOM impedances and quality factors it involved, together with the demonstrated effectiveness of the waveguide-type HOM couplers. As a practical matter, the proximity to the project site of a strong and experienced group of specialists and their willingness to relocate to Newport News were also compelling.

One advantage of the new design was the possibility of greatly reduced energy spread in the extracted beam. To obtain a small relative energy spread ( $\sigma_{\Delta E/E} \sim 2.5 \times 10^{-5}$ ) and comparable relative energy stability, commensurately tight control of rf phase and amplitude in each cavity is required. This task is complicated by the fact that srf cavities operating at about 150 Hz bandwidth (from loaded  $Q$  corresponding to critical matching to the design current) experience microphonics—mechanical vibrations leading to oscillations in their resonant frequency. These oscillations in turn lead to tuning errors of up to  $25^\circ$  in a generally unpredictable manner possessing both random and correlated components. The need to meet tight control requirements without any significant new development

in such circumstances led to a defining characteristic of the CEBAF rf system: Each cavity has its own klystron and low-level control system.

## Recirculation and Beam Optics

The choice of srf technology eliminated the capital and operating costs associated with a multi-hundred-megawatt rf system, but a cursory examination showed the capital cost of a straightforward linac, the technically simplest solution, still exceeded the project's previously established cost boundaries. To meet these constraints, it was essential to adopt beam recirculation—in effect trading costly cavities and cryostats for inexpensive magnets. The concept was simple: Relativistic electrons travel at nearly the velocity of light independent of energy and stay within a fraction of a millimeter (or less than  $1^\circ$  of rf phase at 1500 MHz) of a chosen phase reference point over many kilometers. This idea had never previously been tried on the required scale, though it had been implemented at Stanford's High Energy Physics Laboratory (HEPL) and was a mainstay of operation at MIT's Bates Laboratory.

A recirculating linac sends a beam  $n$  times through a linac section  $1/n$  the length of a full-energy linac by means of  $n$  transport systems tuned to the energy of the  $n$ th path. Each transport system must be unique to accommodate the momentum of the specific beam energy it transports, but in the accelerating sections bunches of electrons of different energy occupy the same spatial locations. As each recirculation path is handled by an independent beam transport system, individual beam-line designs can be evolved to manage synchrotron-radiation-induced degradation of beam emittance and momentum spread. Recirculating linacs thus provide an effective path to high beam energies while allowing preservation of high beam quality.

We can trace the steps from this simple concept to the ultimate shape of CEBAF through a hierarchy of variations and branch points. First, a choice must be made between having accelerating (linac) sections in both legs of a racetrack-shaped layout or in only one. CEBAF opted for both legs, accepting more complex beam transport in return for a shorter length and more freedom of locating the machine on the site. A second decision is whether to operate in "linac fashion," i.e., on the crest of the rf wave without phase focusing, or "microtron fashion," i.e., off-crest with phase focusing. CEBAF chose to operate in linac fashion because it makes optimal use of installed accelerating structures and because phase focusing is not needed with relativistic beam bunches of subpicosecond duration and appropriate precision rf control.

From these decisions flowed the following requirements for the beam transport system(s):

- The linac-to-linac system must be achromatic and isochronous ( $M_{56} < 0.1$  m) on all passes.
- Pass-to-pass tolerance for phase, and therefore path length, is under  $100 \mu\text{m}$ . This type of tolerance calls for "path-length chicanes."

Vertical stacking was chosen, largely for practical reasons. This introduces vertical dispersion, and the choice must be made between constructing individually achromatic vertical bends or correcting vertical dispersion only at the end of the complete arc. CEBAF chose to correct vertical dispersion locally, to make operational, real-time analysis of beam behavior through the arcs as transparent as possible, and to avoid potential synchrotron-radiation-driven excitation of the vertical phase space.

For the same reasons, a philosophy of functional modularity was adopted, resulting in the following breakdown of transport sections from linac to linac: achromatic vertical bend to separate different energies, matching section,  $180^\circ$  horizontal achromatic bend based on a regular lattice operated with matched beam-envelope functions, matching section, achromatic vertical bend back to linac level, with the whole system globally isochronous. The two matching sections downstream of the linacs are long, one containing path-length-adjusting doglegs, the other containing doglegs and beam extraction elements, while the matching regions immediately upstream of the linac sections are short and have no other functions.

A four-recirculation scheme using a pair of 500 MeV linacs was originally proposed and planned, but as cost estimates firmed during evolution of the system design, 100 MeV/linac of acceleration was traded for a fifth recirculation in 1988 as a cost control and optimization measure. Since this change was made when the tunnel was already under construction, it provided the facility with space for adding cryomodules in future energy upgrades.

Finally, a decision was made from the outset to keep the recirculation arc radii large enough to allow later upgrades in energy by avoiding excessive degradation of beam emittance and energy spread. Magnets were designed as low-field, low-current-density devices to minimize power consumption. As a consequence, the existing “4 GeV” beam transport system can be upgraded to 12 GeV by merely replacing power supplies and exchanging a small number of magnets. With a completely new lattice and magnets, the arc tunnel radius is large enough to allow a future upgrade to about 25 GeV (18–20).

## Beam Delivery and Operational Aspects

Simultaneous cw operation of three end stations was a desideratum from the beginning, and with the use of multipass beam recirculation, additional degrees of freedom became available to achieve this goal. Duty-factor-conserving three-beam operation is implemented by creating three interlaced 499 MHz beams at the source (at 100 keV). Spaced apart by  $120^\circ$  of rf phase, they form a 1497 MHz beam in which each bunch has properties, particularly charge, that may differ from its immediately preceding and trailing pair of neighbors, but which repeats every third bunch. With the DC-thermionic-gun-based injector utilized for initial CEBAF operation, this was achieved by sweeping the beam at 499 MHz in a circular fashion over three adjustable slits. Today the same result is achieved by using three independent rf-gain-switched lasers (21, 22) directed at a single photocathode. Simultaneous distribution of three full-energy beams to each of three end stations

is achieved by using properly phased rf deflecting cavities (“rf separators”) operating at 499 MHz following the final pass through the accelerator. In addition, installation of rf separators in the various recirculation paths has made it possible to serve different halls simultaneously with beams of different but correlated energies.

## Beam Polarization

Beam polarization was excluded from the original scope of the construction project. As the scientific program matured during machine design and construction, an immediate need for polarization at or shortly after machine turn-on became obvious. A polarized-source development program was therefore initiated within the framework of commissioning and operations. This effort has kept pace with growing user needs and propelled the Jefferson Lab investigators into a “best-in-class worldwide” position. An account of the approach and results appears below.

## Accelerator Physics

The technical aspects of the conceptual design for a recirculating, srf CEBAF had to be produced within a few weeks. Because this necessity forced quick decisions, many elaborate optimization processes were not conducted once it was clear that a proposed approach would work and would fit the budget. Two main concerns had to be addressed rapidly to maintain credibility for the project: first, that tolerances for regulation of magnet power supplies and alignment were within the state of the art, and second, that the beam was stable against collective phenomena, particularly multipass beam breakup. This phenomenon had been observed as a limitation on the achievable average current at Stanford’s SCA (23) and closely parallels multipass instabilities in storage rings. A beam passing off-axis (due to lattice or injection errors, for example) through a cavity excites deflecting higher-order modes. If these modes have high enough  $Q$ , the beam phase advance, revolution time, and HOM frequency may conspire so that on the next and following passes the excitation is enhanced and the beam deflection increases exponentially—a classic instability. For a single cavity with a simple recirculation layout, a simple analytical model that is readily solved can be created. Even for 320 cavities with a spread in HOM eigenfrequencies, five recirculation passes, and all the intricacies of the lattice, the beam response can be analytically formulated, and numerically solved to obtain growth rates of the instability. Finally, “brute force” simulations were created and evaluated. CEBAF operating currents are 10 to 20 times below calculated thresholds, and no signs of the instability have been observed (24–30).

## Parameter List

Table 1 lists top-level parameters for CEBAF as of early 2001.

**TABLE 1** Principal machine parameters

Energy	5.71* GeV
Average current (Halls A and C)	1–150 $\mu\text{A}$
Average current (Hall B)	1–100 nA
Bunch charge	<0.3 pC
Repetition rate	499 MHz/hall
Beam polarization	>75%
Beam size (rms transverse)	$\sim 80 \mu\text{m}$
Bunch length (rms)	300 fs, 90 $\mu\text{m}$
Energy spread	$2.5 \times 10^{-5}$
Beam power	<1 MW
Beam loss	<1 $\mu\text{A}$
Number of passes	5
Number of accelerating cavities	338
Fundamental mode frequency	1497 MHz
Accelerating cavity effective length	0.5 m
Cells/cavity	5
Average $Q_0$	$4.0 \times 10^9$
Implemented $Q_{\text{ext}}$	$5.6 \times 10^6$
Cavity impedance ( $r/Q$ )	980 $\Omega$
Average cavity accelerating gradient	7.5 MV/m
RF power	<3.5 kW/cavity
Amplitude control	$1.00 \times 10^{-4}$ rms
Phase control	0.1° rms
Cavity operating temperature	2.08 K
Heat load @ 2 K	<9 W/cavity
Liquifier 2 K cooling power	5 kW
Liquifier operating power	5 MW

\*CEBAF has been run for more than 48 hours at 6067.5 MeV. As of early 2001 it was planned to deliver beam for physics experiments at that energy soon.

## PROJECT ENGINEERING AND CONSTRUCTION

### Machine Overview

In February 1987, construction began on an srf CEBAF—a pair of antiparallel srf linacs with a 45 MeV srf injector, supported by a 4.8 kW, 2 K helium refrigeration plant. The linacs are connected by recirculation beam lines, creating a racetrack

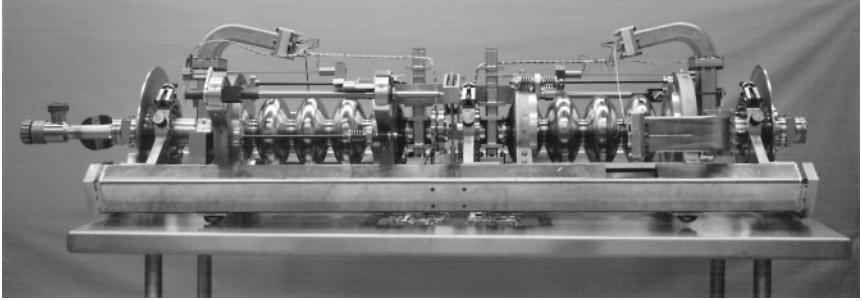


**Figure 3** A CEBAF cavity pair. Each five-cell cavity is 0.5 m long.

machine footprint with a total beam line length over 4.5 km. The performance objectives for the accelerator were final energy between 0.5 and 4.0 GeV, with an eventual goal of 6 GeV informally designated; full-energy beam current up to 200  $\mu\text{A}$ , corresponding to a maximum beam-loading current of 1 mA; cw duty factor; beam rms normalized emittance of 1 mm-mrad; and an rms relative momentum spread of  $2.5 \times 10^{-5}$ . In support of construction, many processing, test, and assembly processes took place in Jefferson Lab's onsite Test Lab, a building inherited from NASA and fitted out for numerous accelerator technology purposes.

Each srf linac consists of 160 accelerating cavities based on a design developed at Cornell University (Figure 3). The Cornell cavity was chosen for both technical and practical reasons: a suitable frequency near 1497 MHz, gradients in laboratory and beam tests in excess of the 5 MV/m needed for CEBAF's 4 GeV final energy (an energy gain of 2.5 MV/cavity/pass), provision for appropriate damping of higher-order modes (HOMs), and readiness for industrial prototyping. The five-cell elliptical cavity structure operates in the  $\pi$  mode and has a fundamental coupler on the beam line at one end and an HOM coupler on the beam line at the other. The elliptical shape yields low peak surface electric fields, a good chemical rinsing geometry, good mechanical rigidity, and resistance to multipactoring of cavities. The HOMs are coupled out of the cavity through two mutually orthogonal rectangular waveguides with a cutoff of 1900 MHz. If undamped, HOMs could have external  $Q$ 's as high as  $10^{10}$ , the unloaded  $Q$  of the modes due to superconducting losses. Resonances in the first HOM pass band ( $TE_{111}$ ) below 1.9 GHz are not damped by the HOM extraction waveguides, but couple out of the fundamental power coupler only. It has been observed that some of these dipole modes are poorly damped, due to self-polarization of the fundamental power coupler. Measurements of HOMs in CEBAF itself and in a similar cryomodule developed for the Jefferson Lab free-electron laser (31) (a spinoff that is briefly addressed later) indicate that loaded  $Q$ 's as high as  $5 \times 10^7$  can exist (below 1.9 GHz) without producing beam instabilities, up to beam currents of 1 mA (5 mA for the free-electron laser). Above 1.9 GHz HOMs are well damped, with typical  $Q$ 's ranging from about 500 to  $10^5$ , representing over four orders of magnitude of damping compared to the fundamental

mode  $Q_0 \geq 2.4 \times 10^9$ . Because the power generated by the beam in HOMs is estimated to be less than 10 mW per cavity, it is inefficient to extract it to room temperature. Special wide-band microwave absorbers are used to terminate the two HOM waveguides in the 2 K helium bath. A special material was developed to provide proper absorption and damping of HOMs (32, 33) because at 2 K most common mechanisms for electromagnetic losses are not present; see, for example, Ziman (34). This material (a ceramic composite of aluminum nitride and glassy carbon spherules) is based on the artificial dielectric model (35) and its dielectric permittivity is independent of temperature over a large range (2 K to 700 K).

To utilize the cavities in a linac configuration, mechanically and operationally manageable cryostat configurations were developed. Cavities were hermetically paired and installed in “cryounits,” four of which make up an 8.25-m-long, eight-cavity “cryomodule.” Each cryomodule is connected to its neighbor by a warm section containing beam vacuum pipe, vacuum pumps and valves, quadrupoles, and steering dipoles. The machine was designed so that each nominally 400 MeV linac would contain 20 cryomodules, with another two and one quarter cryomodules in the injector. The onsite assembly production of cryomodules followed the meticulous processing of industry-produced cavities, and represented a major challenge for the project.

The srf injector provides a high-quality beam that is sufficiently relativistic to stay in phase with the rf and the recirculating beams in the first linac. The injector can provide either a polarized or an unpolarized beam. Following bunching, capture, and initial acceleration sections in the injector, the beam is further bunched and accelerated to just over 5 MeV in a cryounit (quarter-cryomodule), and then accelerated in two cryomodules to 45 MeV for injection (36, 37). Further information on the injector and a more detailed discussion of the polarized source appear below.

The central helium refrigerator, located in the center of the racetrack, supplies 2.2 K, 2.8 atm helium for the cavities and 45 K helium at 4.0 atm for the radiation shields. An end-station refrigerator supplies 4.5 K helium at 2.8 atm for the superconducting magnetic spectrometers in the end stations, supplemented by helium at the same temperature and pressure from the main refrigerator. Both the 2.2 K and 4.5 K helium are expanded by Joule-Thomson valves, yielding 2.08 K at 0.039 atm and 4.4 K at 1.2 atm, respectively. The 2.08 K cavity operating temperature was selected by cost optimization (17): Refrigeration system capital and operating costs rise as design temperature decreases, but rf heat losses in the cavities rise exponentially with temperature.

The rf system includes an individual amplifier chain for each superconducting cavity. Each cavity is phase locked to the master drive reference line to less than  $1^\circ$ , and the cavity field gradient is regulated to within one part in  $10^4$  by an rf control module. A 5 kW, water-cooled, permanent-magnet-focused klystron generates the rf power for each cavity. In service buildings directly above the injector and linacs, the klystrons are arranged in groups of eight over each cryomodule, with each group powered from a common supply.

Projections based on capital cost versus operational complexity showed that between three and six recirculations would be needed for the racetrack-shaped

machine. Four was at first seen as optimum, but further design and cost optimization motivated a move to five passes, requiring a total of nine recirculation beam lines in the arcs linking the linacs. Each line is achromatic and isochronous, provides matching in all phase-space coordinates, and was designed with generous bend radii and strong focusing to minimize quantum excitation.

The definition of an appropriate arc radius required planning beyond the immediate official goal of a 4 GeV machine. Arc size is determined by the maximum energy and the expected beam quality—that is, by the amount of degradation to be tolerated due to synchrotron radiation. It was clear that the experimental users would eventually need energies higher than the expected 6 GeV. All indications with the still-evolving srf technology were that it would eventually support energy upgrades to beyond 20 GeV within the planned linac tunnel length. The radius was set accordingly. As of early 2001, srf technology has indeed evolved successfully; the machine runs near 6 GeV, an initial upgrade to 12 GeV is being planned, and a second doubling of energy to about 24 GeV remains an option for the longer term.

## Building Cryomodules (Design and Process)

To implement the Cornell srf cavity in CEBAF required a focus not only on cavity acquisition and preparation, but also on the cryostat required to keep the cavities at low temperature, the associated beam-line vacuum components, and the infrastructure required for cavity and cryomodule processing, assembly, testing, and installation. The cavity is operated in the  $\pi$  mode and has a fundamental coupler on the beam line at one end and a higher-order-mode (HOM) coupler on the beam line at the other. Specified cavity  $Q_0$  at 2.08 K is at least  $2.4 \times 10^9$ , with 80% of the losses represented by this  $Q$  residual—that is, temperature-independent—and 20% by BCS (Bardeen, Cooper, Schrieffer) losses due to the presence of conduction electrons which are not condensed into Cooper pairs and due to the penetration of a tangential rf electric field several hundred angstroms into the surface of the superconductor.

Industry fabricated the cavities under a carefully formulated and monitored contract. The cavities were made from pure niobium sheet and plate, well inspected for surface defects. Reactor-grade niobium was used for the couplers, but niobium for the “cups” in the five cells was of higher purity, and had a residual resistivity ratio (a measure of niobium purity) of at least 250 (38). This material was deep drawn into cups. Cup edges were machined, the material was cleaned with solvents and acids, and the cups were then electron-beam-welded small end to small end with meticulous quality control. Cavity fabrication included repeated chemical cleaning.

Upon arriving on site, and following inelastic tuning to ensure a flat cell-to-cell accelerating field profile and the correct frequency, cavities underwent cleaning, chemical polishing, and assembly into the hermetically joined pairs in a class 100 clean room. Approximately 100  $\mu\text{m}$  of cavity surface was removed in a two-stage acid-immersion process, followed by several types of precisely specified rinsing.

Some cavities were then individually tested, but the standard test was of the cavity pairs, the most advanced state of assembly prior to installation in cryostats. The pair assembly included ceramic waveguide windows, HOM loads, SMA field probes, and gate valves. Cavity pairs were placed under vacuum and tested in a vertical apparatus at 2 K, with measurements of  $Q$  vs. gradient, maximum achievable field, frequency, input coupling, and reference probe calibration. The integral leak rate of the indium joints in the cavity pairs was measured as the cavity pair was warmed up to room temperature to make sure that the vacuum integrity of the CEBAF beam line is maintained (38a). The cavity vacuum was maintained thereafter (39).

The next stage in the process was assembly of cavity pairs into cryostats called cryounits, four of which were then joined to make one of the 42 cryomodules that were ultimately installed in the accelerator tunnel (20 per linac plus two in the injector, which also includes a cryounit-based “quarter-cryomodule”). These cryostats serve the function of supporting the cavities mechanically, maintaining them at 2.08 K, and keeping the magnetic field at the location of the cavity below 5 mG. The cryounit consists of an outer vacuum vessel, a thermal radiation shield, two layers of magnetic shielding, and a welded helium vessel that encloses the cavity pair. Associated hardware includes superinsulation blankets, helium-vessel supports, tuners, valves, waveguides, bellows, HOM loads and waveguides, vacuum-preserving windows, feedthroughs, and instrumentation. The waveguides, tuner shafts, and instrumentation cables emerge through structures called “top hats” perpendicular to the beam line. Each cryounit was completed by inserting a leak-checked helium vessel into a vacuum vessel and making the necessary electrical and mechanical connections.

Cryomodules consist of four cryounits joined by bridging-ring assemblies, with both cryomodule ends terminated by helium supply-and-return “end cans.” The top hats of each cryomodule’s four cryounits are oriented in a left-right-right-left pattern to provide a high degree of compensation for coupler field asymmetries. Following assembly, some cryomodules were tested in a test facility that includes a radiation-shielded testing room, a pair of 2 kW klystron amplifiers, a waveguide switching system, a control room, and refrigeration connections from the Test Lab’s own small liquid helium facility to both the shield and primary coolant circuits (40, 41).

## Cryogenics System

A particularly high priority early in the CEBAF project was to convert the cryogenics-related aspects of the conceptual design into detailed specifications for the liquid helium refrigeration plant needed to support superconducting operation. The plant came to be called the Central Helium Liquifier, or CHL (42, 43). The CHL’s highest-technology component, its cold compressors, required a long lead time to contract and build, and the completed CHL was expected to require a projected—but as it turned out, underestimated—three years to fabricate and install and two years to achieve the needed 98% availability. Once the CHL was

specified, another aspect of cryogenics became a high priority: building, installing, and commissioning the Test Lab's Cryogenic Test Facility to support cavity and cryomodule pre-installation testing. A third component of the overall cryogenic system was the End Station Refrigerator.

The choice of accelerator, and thus refrigerator, temperature is driven by the operating characteristics of the superconducting cavities. At the very least, superconducting cavities require a cryogenic system to cool them from ambient temperature to an operating temperature below niobium's 9 K superconducting transition point. Maintaining this temperature requires a balance between total cryomodule heat load and cryogenic system heat-removal capacity. Spare capacity is needed as well, for both reliability and cooldown. Even below the transition point, a superconducting rf cavity has two kinds of resistive losses: residual and BCS. Residual losses appear in localized resistive areas where defects or impurities disturb superconductivity. BCS resistance increases with frequency and decreases with operating temperature. Other sources requiring refrigeration include the cryostat static heat leak, the heat dissipated in the input waveguide, and the HOM power generated by the beam current.

The choice of operating temperature affects the BCS component of the cavity  $Q$  and thereby the rf heat load, as well as the refrigeration capital and operating costs. The BCS losses vary inversely with  $Q$ , approximately doubling every 0.2 K. Figure 4 shows the total heat load as a function of temperature. The refrigeration costs vary inversely with the temperature, and capital costs increase with the 0.7

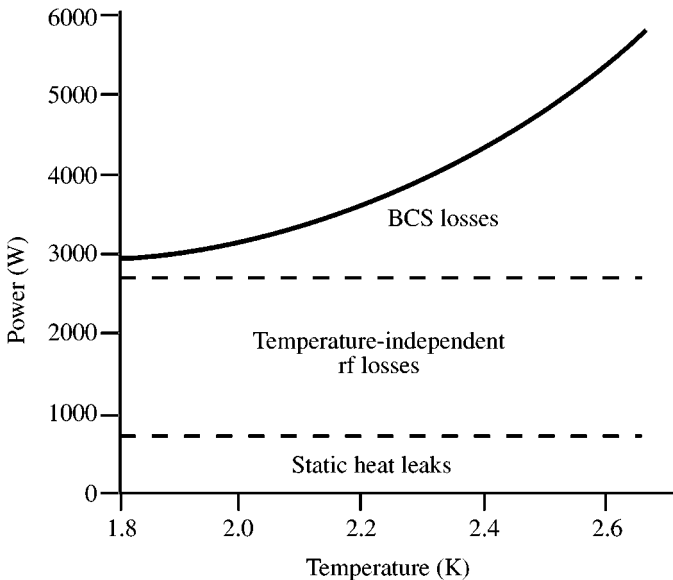


**Figure 4** Total heat load as a function of temperature.

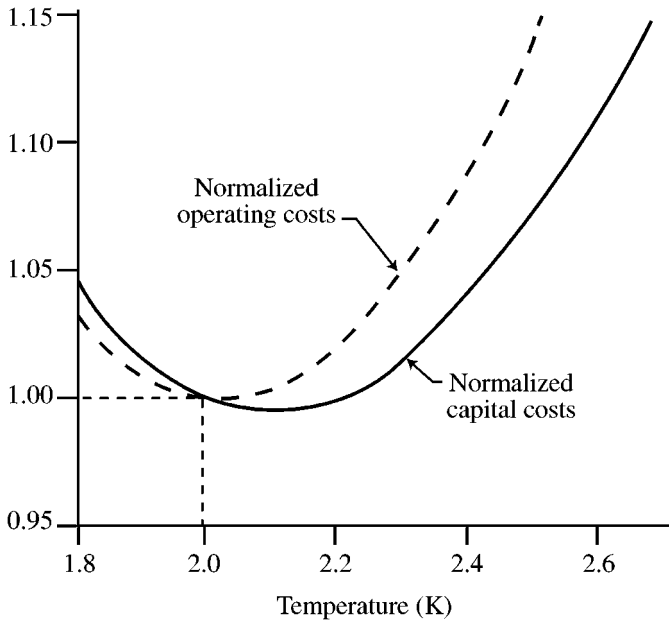


**Figure 5** Normalized costs as a function of the temperature of the superconductor.

power of heat load, while operating costs increase with the 0.85 power. Figure 5 shows the relative variation of construction and operating cost as a function of temperature. The BCS losses, while an exponential function of temperature, are still a small fraction of the total heat load at 2.0 K. The refrigeration capital cost is nearly flat between 2.0 and 2.2 K. Operation below 2.0 K, besides being cost-ineffective, presents a technically difficult vapor pressure of less than 0.031 atm. Operating above 2.5 K would allow deleting one stage of vacuum pumping, but would raise costs unacceptably because of BCS losses. An operating temperature of 2.08 K was thus chosen as a cost optimum (17).

The optimal operating range of CEBAF is 2.0 to 2.5 K. The distribution system was optimized for 2 K with a flow safety factor twice the calculated heat load. Since future increases in cavity gradients would tend to lower the optimum operating temperature, this would permit future beam energy increases without relatively expensive distribution-system replacement. The CHL was specified as a 2 K unit, thereby providing two advantages: a safety margin of 0.2 K to 0.5 K for the pressure drops that could occur during commissioning, and heat exchanger compatibility with possible future upgrades. It was later recognized that there was major loss in heat transfer as one crossed lambda; therefore 2.17 K is an upper limit (44).

The CHL now comprises three pairs of compressors, the main cold box that produces 45 K and 4.5 K refrigeration, the subatmospheric cold box that lowers

the temperature from 4.5 K to 2.0 K, 113,550 liters of liquid helium storage (including 67,600 liters in the cryomodules themselves), and 40,000 gal of liquid nitrogen storage. A pair of transfer lines provide two parallel cooling loops to each cryomodule, vary from 6 inches to 16 inches in diameter, and have a total length of 4500 ft (45).

There were many technical failures during the CHL construction and commissioning. The primary areas were the cold compressors and cold turbine (46). As soon as the 4.5 K coldbox was partially operational in February 1991 the north (i.e., first) linac was cooled down and reduced-energy beam operation started with the assistance of warm vacuum pumps. In the spring of 1994 the refrigerator was modified for cold compressor operations, which then started in April 1994 at 2.3 K and the following month at 2.1 K (sub-lambda). At the end of two years of operations, the srf and cryogenics systems were among the most reliable at CEBAF. Neither linac has ever been warmed up in its entirety since their cooldowns in February 1991 and March 1993.

## RF Systems

The requirement for  $2.5 \times 10^{-5}$  rms relative energy spread necessitates strict control of the phase and amplitude of the 1497 MHz accelerating field (47). If unregulated, the amplitude and phase fluctuations would differ from cavity to cavity due to different noise sources along the tunnel and differences in the loaded  $Q$  of the cavities. Therefore, separate feedback channels for each cavity are necessary to meet the stringent requirements for amplitude and phase stability. For cost reasons, the controllers for phase and amplitude are operated at power levels below 100 mW. Such a scheme requires a separate klystron for each cavity, with each providing a maximum drive power of 5 kW (48–53).

The rf system consists of a stable master oscillator (54), a phase distribution system (55, 56), and the individual drive chains for the 320 superconducting cavities in the linacs and for the three drive lasers, two choppers, a buncher, a capture section, and 18 superconducting cavities in the injector (57). The drive chains, one per cavity, consist of the rf control module (58), the high-power amplifier (HPA) containing the klystron, and the waveguide feeding the cavities. A probe signal from each cavity is fed to its control module, thereby closing the feedback loop. Service buildings at grade level above the tunnel house the racks for the rf controls.

The klystron is a 5 kW, cw, four-cavity, water-cooled microwave amplifier operating at 1497 MHz. An integral permanent magnet provides beam focusing. A modulating anode is incorporated to reduce the klystron beam power to a value producing the rf power required by the accelerator cavity at a given time. This control of klystron beam input power results in global reduction of accelerator primary input (“wall plug”) power. The small signal gain of the klystron is 38 dB at minimum. Nominal saturated rf output is 5 kW; proper operation of the accelerator requires klystron power well below this level.

Specialized rf systems are used for beam diagnostic purposes, and for beam production and extraction. The beam position monitors, beam current monitors, and beam phase monitors detect beam-generated 1497 MHz rf signals after down-conversion to a suitable intermediate frequency: 0.1, 1, and 10 MHz for the various beam position monitoring systems (59–61), 1 MHz for the current monitors (62), and DC for the relative phase monitors. As discussed in the next section, rf systems based on the third subharmonic of the fundamental, 499 MHz, are used to produce, extract, and separately control the beam current going to each of the three experimental halls.

## Beam Transport

Six subsystems make up the beam transport system of—and define the modular design approach for—the five-pass CEBAF accelerator: injector optics, linac lattices, spreaders, recombiners, recirculation arc beam lines, and extraction region (63–66). A conceptually simple and operationally reliable system was desired. Two main requirements drove system design. First, maximum stability of the beam was required against collective effects such as beam breakup. As discussed above, multipass regenerative beam breakup can severely limit current in superconducting linacs due to the inherently high  $Q$ 's of transverse deflecting modes of the rf cavities. In the Stanford recyclotron (23), beam breakup had limited the beam current to tens of microamperes, and this instability was the subject of extensive simulation during CEBAF's conceptual design phase. Second, degradation of beam quality had to be minimized. Phase-space dilution could arise from synchrotron radiation excitation during recirculation or through optical errors such as mismatches of the beam phase space, distortions generated by optical aberrations in the beam lines, and perturbations due to imperfections in bending and focusing fields (67–75).

Injection into the first linac was at first predicated on a simple horizontal chicane to guide the 45 MeV beam around arc-to-linac reinjection elements, but during detailed design it became clear that this geometry required modification to suppress bunch lengthening. An isochronous chicane, with embedded quadrupoles used for dispersion modulation/longitudinal phase-space management, was therefore implemented.

The beam transport system of either linac consists of a series of  $12\frac{1}{2}$  FODO cells, with two embedded cryomodules in each of the first ten cells. The half-cell length is 9.6 m; the cryomodule length of 8.25 m allows a 1.35 m intercryomodule warm region for beam focusing, steering, and monitoring devices. The recirculation lines between the two linacs are tuned to provide imaging of the beam phase space from linac to linac. As a consequence, the linac pair behaves on each pass much like a single contiguous linac of 25 FODO cells with 40 embedded cryomodules and ten vacant cryomodule slots (available for energy upgrades).

Optically similar spreaders and recombiners enable beams of different energy to transit the individually energy-tuned arc beam lines. Beams leaving a linac are spread via differential vertical bending, according to energy, into the separate arc

lines. In the recombiner, a mirror image of the spreader, individual beams from the lines are phase matched to the next linac.

The nine arc beam lines—five in the first arc, four in the second—are designed to avoid degradation of beam quality through error sensitivity, synchrotron radiation excitation, or optical aberrations. This implies two lattice constraints. The first is that the beam line lattices be achromatic, isochronous, imaging, and provide a total beam-path length that is an integer multiple of the rf wavelength. These features facilitate both transverse and longitudinal matching between linacs and ensure that no phase-space dilution occurs. The second constraint is minimization of synchrotron-radiation-induced phase-space degradation. The radiation-induced energy spread  $\sigma_E$  and emittance increase  $\Delta\varepsilon$  that occur when a beam is bent by  $180^\circ$  are given by

$$\sigma_E^2 = 1.182 \times 10^{-33} \text{ GeV}^2 \text{ m}^2 \frac{\gamma^7}{\rho^2}$$

$$\Delta\varepsilon = 1.32\pi \times 10^{-27} \text{ m}^2 \text{ rad} \frac{\gamma^5}{\rho^2} \langle H \rangle.$$

Here

$$\langle H \rangle = \frac{1}{L} \int_{\text{bends}} ds \left( \frac{1}{\beta} \right) \left\{ \left[ \eta^2 + \left( \beta\eta' - \frac{1}{2}\beta'\eta \right)^2 \right] \right\},$$

with  $\gamma$  = the beam energy divided by the electron rest mass,  $L$  = orbit length in bending magnets,  $\rho$  = orbit radius in bending magnets, and  $\beta(s)$  and  $\eta(s)$  being the horizontal beam optical functions as functions of longitudinal coordinate  $s$ . The induced energy spread is a function of the bending radius only, but the emittance increase may be controlled, in part, by the choice of lattice functions (64).

The beam is extracted at the end of the south linac and transported to the experimental halls. A 1/3-harmonic rf separator system permits splitting of the three interleaved bunch trains and simultaneous operation of all three experimental halls. Beam energy for each line can be taken from any of the five-pass energies; the 499 MHz rf separators used for this purpose are based on a quarter-wave resonator design (76–78). For a full-energy “three-beam” split, one bunch train is phased with the zero crossing of the deflecting field in a separator immediately downstream of the accelerator. This bunch train is thus undeflected and propagates forward through the field-free (central) aperture of a three-aperture Lambertson septum (79). The other two trains are then deflected at equal angles in opposite directions into conventional septum magnets, which subsequently steer the bunch trains into appropriate high-field apertures of the downstream Lambertson. The beams are thereby directed to the desired experimental hall.

Multiple-energy delivery to multiple end stations is provided by performing a “two-beam” split within the accelerator (78, 79). Separators embedded in “extraction regions” in each recirculation path at the end of the second linac are phased to provide the maximum deflection to the bunch train of interest. It is deflected across

a sequence of current sheet septa, and extracted to the transport lines to the halls. The other bunch trains,  $120^\circ$  out of phase with the maximum, are both deflected in the opposite direction, both with identical amplitude (equal to half that of the kick driving the extracted beam). They do not, as a result, enter the septum chain, and instead propagate forward into the recirculation arc, where the imposed orbit error is corrected and the beam is transported for further acceleration.

The transport lines to the halls are conceptually identical to one another: Downstream of the Lambertson, each has a matching section, a bending section to direct the beam toward the hall, and final matching to the target.

The magnetic elements required by the optics design are numerous but not, in general, extraordinary (80). The 2267 individual magnets include 1047 corrector dipoles, 390 major dipoles, 707 quadrupoles, 96 sextupoles, 26 septa, and a Lambertson septum. All were magnetically mapped in the Test Lab before installation (81) and aligned at final installation (82).

## Control System

Until the early 1990s, CEBAF developed its original control system, TACL (Thaumaturgic Automated Control Logic). This was a “classic” approach involving distributed front-end computers performing data acquisition and control as well as dedicated console computers for operator displays. Client processes executed on workstations, typically displaying machine data in a graphical format. Communication between the front-end computers and client processes utilized a “star” process, mediating communications between all front-end computers and clients of the control data originating on the front-end computers. Communication between the star and other processes was based on named data (83).

Problems were encountered, however, in scaling TACL to the full CEBAF machine during the period when installation and commissioning were progressing in parallel. A switch to EPICS (Experimental Physics and Industrial Control System) was undertaken, and was accomplished incrementally during machine commissioning, starting with the linacs and progressing to the injector. EPICS is a control system toolkit jointly developed by collaborating laboratories in the United States and Europe. It too follows a “classic” model and is similar to TACL in topological design and network communication protocol, with operator display computer nodes decoupled from the data-acquisition and control nodes, with communication between display and control nodes based on making named requests for data, and with data being passed on change of value (84). TACL’s use of a central communications process allowed the integration of both systems’ network communications in that process, in turn precluding any need for software changes to support intersystem network communication during the changeover.

This “migration” to EPICS took place in a controlled, evolutionary manner, with new and old systems operating concurrently (85, 86). Existing CAMAC hardware was preserved by adding a CAMAC highway serial link to VME. Software is distributed among three tiers of computers: workstations and X terminals for

operator interfaces and high-level applications, VME single-board computers for distributed access to hardware and for local processing, and embedded processors where needed for faster closed-loop operation. In some cases, multiple VME processors transparently access a single serial highway for improved performance.

This still-evolving system (87–90) has demonstrated the ability to scale EPICS to controlling 35,000 devices, including hundreds of embedded processors, with control distributed among approximately 80 VME processors executing more than 250,000 EPICS database records. A database is used to deal with the control system's large size, providing data-management capabilities for both low-level I/O and high-level machine modeling. A control-system-independent callable interface permits access to live EPICS data, data in other Unix processes, and data in the database.

## COMMISSIONING, MACHINE PERFORMANCE, AND SCIENCE

Commissioning activities started concurrently with construction. Interim shielding and walls were placed in the tunnel to allow beam operations in the machine front end while installation activities proceeded further downstream. The first phase—the Front End Test, involving the two and one-quarter cryomodules of the injector—certified the capability of the low-level rf system to control the cavities at the required tolerances in an operational installation (57, 91–93). In a recirculation experiment using a temporary beam transport system, the Front End Test also confirmed that the multipass beam-breakup threshold was above operating currents (30). In 1992, later tests commissioned the first half of the first linac including high beam loading (94), and eventually a portion of the first arc (95), followed by full tests of both the first linac and a portion of the first arc.

Commissioning of the entire first pass was completed, and the milestone of bringing one-pass beam to Hall C was accomplished, in the second quarter of fiscal year 1994—precisely according to the project schedule established in 1988 (96). The halls were scheduled to come on line in sequence. Commissioning higher passes thus proceeded in parallel with equipment tuneup in Hall C. The full design energy of 4 GeV from five passes was achieved in May 1995 (97). By early 1996, a single-pass energy of 1 GeV had been achieved in the two linacs, 25% above their combined nominal specification of 800 MeV. The machine was providing multipass beam to users and had produced multiple beams (98, 99). Work on raising energy took precedence over demonstrating beam current since most experiments in their early stages were not capable of handling full-power beam. By fall 1997, with physics experimentation well under way, the machine was operating essentially as designed, and full capacity of 4 GeV at 200  $\mu$ A was delivered (100, 101). In 1998, simultaneous three-hall operation achieved the same operational reliability as single-hall running. The CEBAF accelerator has achieved a small extracted energy spread (102), as it was designed to do.

## Polarized Source Development

As noted earlier, polarized beam was a desire from project inception, and as the user program matured during machine design and construction the emerging importance of this capability motivated an aggressive program of source development. These activities proceeded in parallel with machine commissioning and resulted in the initial availability of polarized electrons soon after the advent of full machine operation (103).

The polarized electron source went through several iterations between its initial operation in early 1997 and early 2000. The original source was constructed at the University of Illinois (104). The electron gun of this source, operated at 100 keV, was very similar to the original SLAC PEGGY II polarized source, incorporating only very minor modifications. The gun was mounted vertically, with the beam brought into the plane of the accelerator by a double-focusing  $90^\circ$  dipole magnet. A pair of solenoids after the dipole restored a round beam. A z-style spin manipulator, originally proposed at Mainz, was incorporated (105). This spin manipulator employed two double-focusing electrostatic bends and eight solenoids, and thus proved a difficult system to steer the beam through. A 100 keV Mott polarimeter was provided immediately before the polarized beam entered the main injector beam line.

The unique laser used with this polarized source was developed in-house. It was a diode-laser-based oscillator-amplifier system. The diode-laser oscillator was rf gain-switched to produce an optical pulse train at either 1497 MHz or 499 MHz (21, 22). The nominal optical pulse width from the laser was about 55 ps. By producing this pulse train, much of the loss associated with beam chopping was avoided. However, the photocathode in this setup was over 11 m from the chopping apertures, and at higher average currents, space-charge-induced bunch lengthening still produced chopping losses. Accordingly, a low-power prebuncher was added midway between the cathode and the chopping apertures. With this prebuncher, it was possible to reduce the chopping losses to small values, even at 100  $\mu\text{A}$  average current.

This original polarized source was put into service early in 1997. During its initial operation, the gun delivered up to 30  $\mu\text{A}$  cw beam from a conventional gallium arsenide photocathode over a period of six weeks. The operational lifetime of the photocathode was acceptable at these low average currents, but it was clear that, to meet the high-average-current, high-polarization requirements of the experimental physics program, the cathode operational lifetime would need to be much longer. One clear observation relating to the operational lifetime was that as the average current from the polarized gun was increased, the beam-line vacuum became steadily worse. Sensitive Geiger counters placed along the beam line in the vicinity of the gun indicated that there was significant beam loss throughout this area.

Initially it was very difficult to understand the mechanism for this beam loss, since the photocathode, with a diameter of 12.8 mm, was illuminated by a laser beam that was about 0.2 mm in diameter. The problem was finally understood as

being due to recombination light reaching large-radius areas of the photocathode, coupled with severe overfocusing in the gun. Photoemission from the large-radius portions of the cathode produced electrons which followed extreme trajectories, striking the vacuum wall in the vicinity of the photocathode. This degraded the vacuum through electron-stimulated desorption. Once the origin of the cathode degradation was understood, the problem was corrected by a number of measures, namely, (a) deadening the quantum efficiency of the photocathode at large radius, (b) reducing the focusing in the electron gun, (c) dramatically increasing the pumping speed in the vicinity of the photocathode by adding a large NEG (nonevaporable getter) pump array, (d) eliminating all short-focal-length beam-line elements (e.g., the  $90^\circ$  dipole and the z spin manipulator), (e) increasing the bore of the beam-line vacuum in the vicinity of the polarized gun, and (f) adding an NEG coating on the inner surface of the beam tube following the gun. These changes, which were done in stages, made a dramatic improvement in the photocathode lifetime. The largest improvements were made by deadening the quantum efficiency at large radius and by providing massive pumping in the vicinity of the cathode.

These changes to the polarized source have led to the present system, which has two horizontal polarized guns, each mounted at a  $15^\circ$  angle to the main injector axis. Beam from one or another of these guns is deflected onto the main injector axis by an anastigmatic air-core dipole, which has a focal length of about 3 m in each plane. The laser system is composed of three 499 MHz diode lasers. Each laser provides beam to one end station. Switching beam delivery from one to the other gun requires less than 1 h and is accomplished completely remotely.

At present the operational lifetime of the photocathode is limited solely by ion backbombardment. Thus, the most suitable measure of the cathode life is not the number of hours of operation but rather the total charge delivered per illuminated area. The operational lifetimes of thin, strained gallium arsenide cathodes now routinely exceed  $10^5$  C/cm<sup>2</sup>. Further vacuum improvements to increase this lifetime are planned. The nonilluminated areas of the photocathode do not degrade during operation. Consequently, when the quantum efficiency has dropped to the point where it is no longer possible to deliver the required current, the laser spot is moved slightly on the cathode, and beam delivery is resumed. Most, although not all, of the ion backbombardment damage is recovered by a cycle of cathode heat treatment and reactivation with cesium and nitrogen trifluoride.

Currently, all operation is with thin, strained gallium arsenide photocathodes, which operate at about 850 nm wavelength. These commercially purchased cathodes provide polarization between 70% and 80%. Unfortunately, they show relatively large linear strain in the crystal plane, as well as the uniaxial strain perpendicular to the crystal plane which provides the high polarization. This linear strain is the origin of relatively large helicity-correlated position and intensity changes. Jefferson Lab was the first to demonstrate the successful control of these large helicity-correlated effects at a level that permitted small parity-violation effects to be measured—as was crucial in the HAPPEX experiment mentioned below among the highlights of Jefferson Lab physics results.

At present the electron polarization is measured at 5 MeV with a Mott polarimeter (106). Spin manipulation is provided by a large-aperture Wien filter. It was recognized some time ago that a large number of energy combinations in the end stations would provide simultaneous perfect longitudinal polarization to any two halls, and nearly perfect longitudinal polarization to all three halls, for a single Wien filter setting (107). We have successfully delivered longitudinal polarization to all three halls on several occasions. The combination of data from the high-precision Mott polarimeter with data from polarimeters in the experimental halls has allowed fairly complete spin tracking through the accelerator, and a way to verify the absolute beam energy. Polarization manipulation and control, and the ability to deliver good polarization to more than one hall simultaneously, are essential because the experimental program requires polarization in more than one hall for the majority of the scheduled time. When an experimental hall does not require polarization, the laser wavelength is changed to about 780 nm to take advantage of the higher quantum efficiency. Simultaneous delivery of highly polarized and nominally unpolarized beam has become routine.

## Machine Performance

CEBAF now runs reliably for extended periods, having produced 5614 hours of beam for users in FY2000. The system operates with availability of order 70% (Figure 6), and the installed srf base exceeds, on average, system design goals for cavity intrinsic and external  $Q$  (Figures 7 and 8) and gradient (Figure 9). The availability of linac performance surpassing initial design goals has proven a significant motivation for efforts to extend the machine energy beyond the initial 4 GeV goal. Initial cavity performance provided a reliable five-pass energy in excess of 5 GeV, limited by electron field emission. To reduce the field emission and boost the operational energy, in situ processing of the cavities was begun (100), leading to a 6 GeV test in 2000 and regular operation at 5.7 GeV.

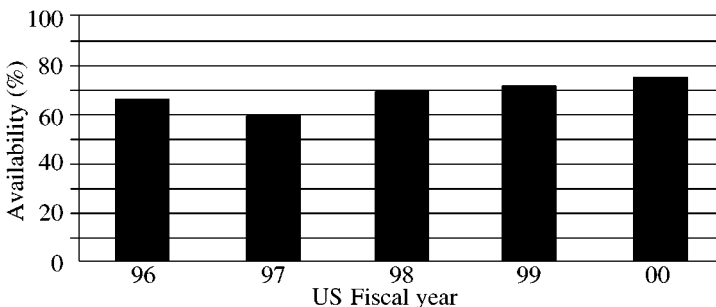


**Figure 6** Machine availability.

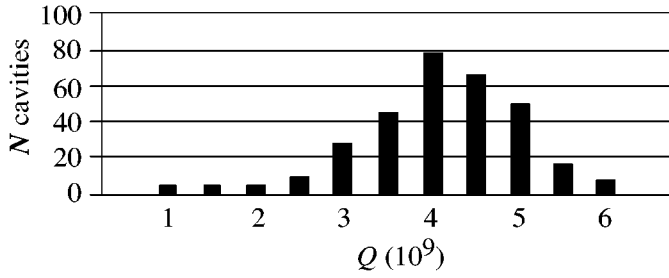


**Figure 7** Cavity  $Q$  distribution.

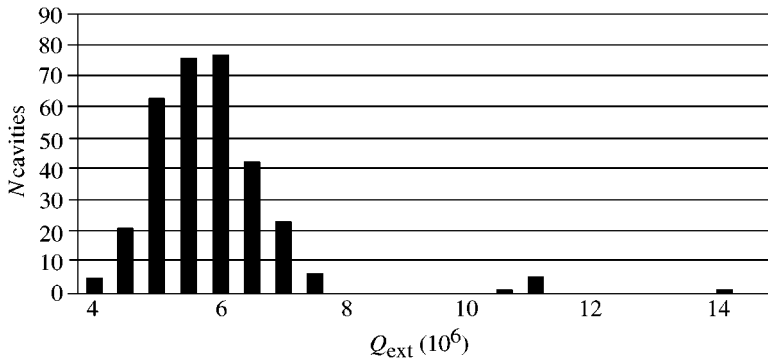


**Figure 8** External  $Q$  distribution.

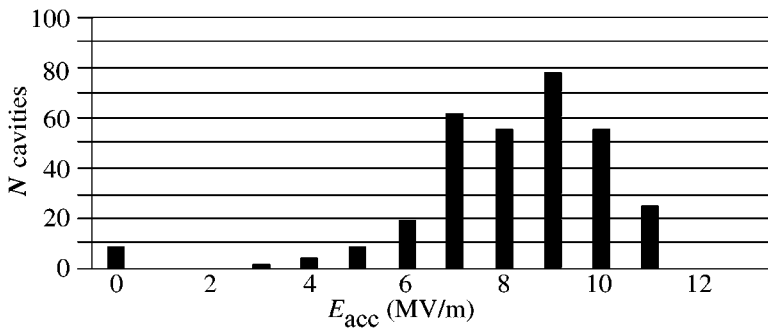


**Figure 9** Gradient distribution (J. Benesch, personal communication).

## Physics Results

Some of the highlights of the CEBAF physics program up to 2000 include the following:

- The proton's electromagnetic structure (108). For more than 20 years it has been assumed, based on the available data, that the charge and magnetization distributions in the proton are proportional to one another. New data from Hall A show that the distributions are not proportional, leading to a reexamination of the dynamics governing the proton's quark wavefunctions.
- Strange quarks in the proton (109). Virtual strange quark–antiquark pairs can exist within the proton. In hadronic language, the proton can dissociate into a virtual hyperon–strange meson system. In quark language, strange–antistrange pairs are constantly being made virtually by gluon-mediated interactions inside the proton. In either case, one expects a substantial probability of strange quarks and a corresponding contribution to the charge and magnetization distributions of the proton. (A predicted strange-quark contribution of 10% of the proton magnetic moment is typical.) To disentangle this contribution from the dominant effects of the u and d quarks requires the use of the weak interaction (Z exchange) as a probe. The HAPPEX experiment in Hall A shows that the actual contribution is considerably smaller than expected in most models.
- Missing excited states of the nucleon. If the proton is made of three spin- $1/2$  quarks, then its “atomic” excitation spectrum must contain a certain number of levels with certain quantum numbers. More than half of the low-lying states needed to test this basic picture are missing, and the data are consistent with models in which a di-quark (quark pair) and a quark, rather than three independent quarks, describe the basic degrees of freedom of the proton. Recent data from Hall B's CEBAF Large Acceptance Spectrometer are clearly of a quality sufficient to perform the phase-shift analysis that will be essential to identify the missing states predicted by three-quark models (if they are present) and already show that strength in the region where these states are expected with a large amount of the decay occurring via omega emission. This is consistent with theoretical predictions for the location of the states and with the fact that they have not been seen in earlier experiments (which involved pion excitation).
- Probing the limits of standard nuclear physics (110–112). The deuteron is not a spherical nucleus. In the standard proton–neutron picture of this simplest nucleus, its shape is largely determined by pion exchange, which leads to strong noncentral (namely “tensor”) interactions between the nucleons. Although it is clearly correct at large distances, many expected this description of the N–N force to break down as one looked at the deuteron with finer and finer spatial resolution. Data from experiments in both Hall A and Hall C have determined the shape of the deuteron through elastic electron–scattering measurements to high momentum transfers corresponding to distances of order the proton radius and have shown no departure from standard nuclear physics.

## Spinoffs and Parallel Efforts

The institutional knowledge base and infrastructure that have evolved with the construction of CEBAF enable Jefferson Lab to pursue scientific and technological initiatives beyond the scope of those initially envisioned. The performance of srf technology in general and the CEBAF accelerator in particular has been both promising and robust enough to encourage parallel and spinoff efforts within the institution. The most visible of these involve application of srf technology to accelerator systems for free-electron lasers (FELs) and for proton accelerators to produce neutrons for research in materials science.

## The Infrared Demonstrator Free-Electron Laser

Well before the full commissioning of CEBAF, initial experience with CEBAF srf systems was sufficiently promising that investigations commenced on the use of an srf accelerator as the electron-beam “driver” for an FEL (113). Considerable interest consequently arose during the construction phase of CEBAF concerning the possibility of using the accelerator in this manner (114–116), but, due to significant constraints both technical and organizational, attention soon shifted to the concept of a stand-alone srf-based FEL driver accelerator (117). This interest led to the construction of the Jefferson Lab IR Demonstrator FEL, a cw system at 1 kW average power driven by a 35–48 MeV, 5 mA srf linac (118). This machine has produced average cw coherent light power of up to 1.72 kW (119) using essentially CEBAF-standard rf and beamline components.

Energy recovery is the key to this implementation of srf. In this technique, the electron beam used to drive the FEL is recirculated out of phase with the drive linac rf, with the beam power thereby returned to the srf structure, maintaining the fields that accelerate subsequently injected electrons. The resulting system requires virtually no rf power beyond that used to establish and maintain cavity fields and to replace power extracted by the FEL itself. Critical to the use of this technology is appropriate management of the beam longitudinal phase space to provide energy compression during energy recovery (120, 121), to avoid excessive beam quality degradation and beam loss.

In addition to high-power lasing with energy recovery, the FEL user facility (122) has supported a variety of investigations in fundamental and applied science and technology. Progress has been rapid, with numerous accomplishments including

- lasing at variable user-defined wavelengths around 3, 5, and 6  $\mu\text{m}$ ,
- third- and fifth-harmonic lasing (at powers of up to hundreds of watts) at 1  $\mu\text{m}$ ,
- production of short-pulse (300 fsec rms), high-brightness beams of X-rays via Thomson scattering, and
- service to the experiments of numerous materials science and surface science users.

The success of the IR Demo FEL has led to funding—by the U.S. Navy and Air Force as well as other agencies—of an upgrade of the system to 10 kW in the IR and 1 kW in the UV. The upgrade, under construction as of 2000, increases the IR output light power by doubling the FEL extraction efficiency and increasing the drive electron beam power by almost an order of magnitude (Benson and colleagues, to appear in the proceedings of the 2001 Free-Electron Laser Conference; Douglas and colleagues, to appear in the proceedings of the 2001 Particle Accelerator Conference). The electron beam power is raised by increasing the driver linac energy from  $\sim 50$  MeV to as high as 210 MeV and doubling the source current from 5 to 10 mA (123). Initial operation of the upgraded IR system is expected in the fall of 2002, with operation of a UV system, driven by the same accelerator, in the following year.

### SRF Systems for the Spallation Neutron Source

Advances in the technology of proton acceleration—particularly qualitative improvements in the ability to bunch and accelerate high-intensity, low-energy beams—have stimulated the emergence of new applications for high-average-power proton accelerators that require srf acceleration systems for efficient implementation. The expertise developed during the design, construction, and operation of CEBAF has positioned Jefferson Lab to contribute to such projects. The most advanced of these is the Spallation Neutron Source (SNS) project under construction at the Oak Ridge National Laboratory in Tennessee, a major initiative in the use of neutrons as probes for basic materials research in biology, medicine, and industry.

As the U.S. leader in implementation of superconducting rf technology, Jefferson Lab is participating in the SNS project by building the superconducting accelerating elements and the superfluid helium refrigeration and distribution system. As of early 2001, the design of these systems was complete and construction was getting under way. This project requires more than a straightforward replication of the CEBAF cavities scaled to 805 MHz. Power delivered to the beam in each cavity is raised from less than 10 kW to more than 300 kW, which requires different solutions to the problem of coupling rf power into superconducting resonators. In addition, the cavities must be optimized for particle velocities well below the speed of light, which requires revisiting the problems of multipactoring and vibrational detuning control that are already solved for electron acceleration. The development program to address these issues, carried out in collaboration with many of the members of the international srf community, is well advanced.

### FUTURE DIRECTIONS

Evolving physics desiderata have driven and continue to drive CEBAF's evolution. As of early 2001, the 4 GeV machine envisioned in 1986 operates at nearly 6 GeV, with an upgrade to 12 GeV expected, and with support emerging for another doubling to about 25 GeV later. The science driving the 12 GeV upgrade has been

reviewed by the Jefferson Lab Program Advisory Committee and is documented in a white paper (124). The proposed upgrade allows breakthrough programs to be launched in two key areas:

- The experimental observation of the QCD flux tubes that cause confinement. Theoretical conjectures, now confirmed by lattice QCD (quantum chromodynamics) simulations, indicate that the most spectacular new prediction of QCD—quark confinement—occurs through the formation of a string-like “flux tube” between quarks. This conclusion (and proposed mechanisms of flux-tube formation) can be tested by determining the spectrum of the gluonic excitations of mesons.
- The measurement of the quark and gluon wavefunctions of the nuclear building blocks. A vast improvement in our knowledge of the fundamental structure of the proton and neutron can be achieved. Not only can existing “deep inelastic scattering” cross sections be extended for the first time to cover the critical region where their basic three-quark structure dominates, but also measurements of new “deep exclusive scattering” cross sections will open the door to a new, more complete characterization of these wavefunctions by providing direct access to information on the correlations among the quarks.

In addition to opening up these qualitatively new areas of research, the 12 GeV upgrade will open important new research opportunities in key areas already under investigation.

The technical basis for the upgrade is the ongoing development of a cryomodule whose key elements are a 40% increase in active length and extreme attention to maintaining high  $Q$  values at accelerating fields exceeding 20 MV/m. Thus, this upgrade is not only important to completing the picture begun with our current experimental program in nuclear physics, but the R&D in srf and expertise in related technologies that enable it are critical for many of the facilities under way or planned in the larger science community.

## Basic Design Considerations for Higher Energy

The CEBAF layout serves as a model for a cw electron accelerator with higher energy: superconducting accelerating cavities, beam recirculation with a moderate number of passes, and multihall operation. Basic design considerations for higher energy include the following:

- The energy accessible with such a device is the product of average accelerating gradient, installed active length, and number of passes. With values for these parameters, respectively, of 15 to >20 MV/m, 160 to 300 m, and 5 to 7, the targeted energy range is covered, and key questions emerge concerning limitations and optimizations.
- In a superconducting linac, the required rf power is determined by the specified beam power and by the degree to which microphonics is controlled, and is otherwise largely independent of detailed parameter choices.

- Assuming some degree of HOM damping and design currents of a few tens to about  $100 \mu\text{A}$ , multipass beam breakup is not a limitation, and will not significantly enter the tradeoff between voltage gain and number of passes.
- Depolarization of polarized beams is not an issue in a machine with CEBAF-like topology.
- A key cost optimization issue is the tradeoff among length, gradient, postulated quality factor  $Q$ , and the budgeted cryogenic power. Once gradients in excess of  $12 \text{ MV/m}$  are available, achieving  $Q$  values above  $5 \times 10^9$  at the operating gradient is essential to contain cryogenic system cost.

In addition, a central performance issue, particularly at the upper end of the energy range, is degradation of beam quality due to synchrotron radiation. The increase in energy spread is solely a function of energy and magnetic field strength, while the emittance growth, dependent on the same parameters, is further modified by the focusing properties of the transport system. In a green-site machine design, the arc radius is thus an important open parameter. For CEBAF it is fixed by the existing enclosure to approximately 80 m.

### CEBAF 12 GeV Upgrade

Mindful of these general considerations, the following 12 GeV upgrade plan has been adopted:

1. Complete R&D for a seven-cell cavity (Figures 10 and 11) and a cryomodule that can exceed 100 MV energy gain.

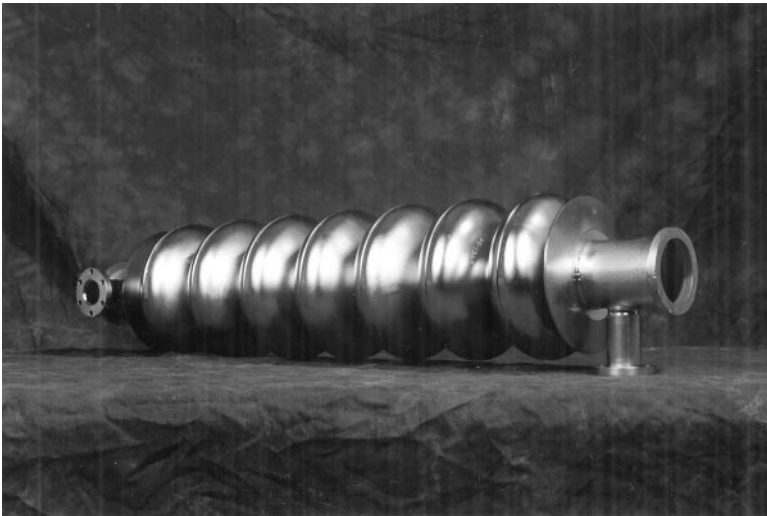


**Figure 10** Prototype seven-cell cavity.

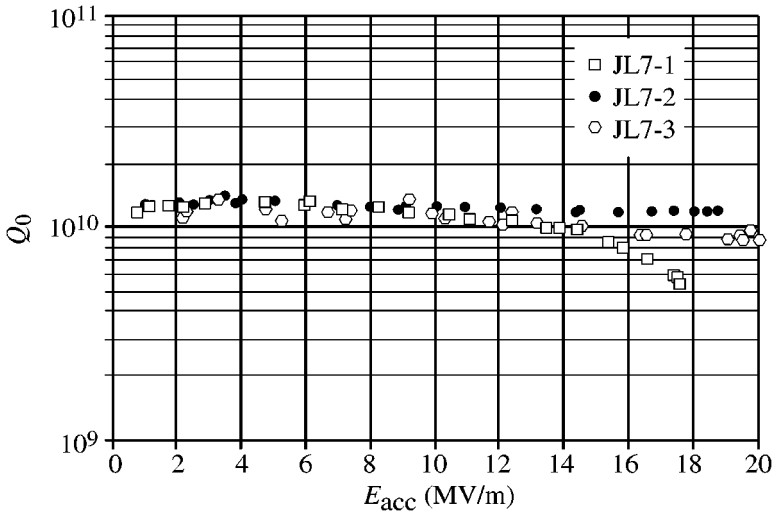


**Figure 11** Performance of prototype seven-cell cavities.

2. Upgrade the existing cryoplant (5 kW at 2 K) to 10 kW.
3. Upgrade magnet power supplies in arcs 1 through 7.
4. Modify magnets in arcs 8 and 9, and add a tenth arc and a fourth experimental hall. These modifications and additions maintain the existing lattice layout (125).
5. Maintain beam power at 1 MW.
6. In the ten empty slots in the linacs, add new cryomodules: >100 MV is the design goal, representing a gradient of about 20 MV/m.
7. If the cryomodule goals are not fully met, replace the weakest two to four cryomodules in the present machine with new ones.

Figure 12 and Table 2 illustrate the plan for 12 GeV.

### Comparison with Electron Linac for Europe (ELFE)

This upgrade plan should be compared with the other possibilities for CEBAF-like accelerators being discussed around the world. The two ideas for which the greatest amount of work has been completed have been supported under the project name Electron Linac for Europe (ELFE). The ELFE project originated in France at Saclay, where the first proposal had a 10 GeV nuclear physics machine, and now is centered at CERN, where present thinking is focused on a 25 GeV seven-pass accelerator. The initial proposals, which have evolved over the years in concert with the increase in performance of superconducting cavities, have generally involved a single linac with three or four recirculations, and with final energy roughly twice

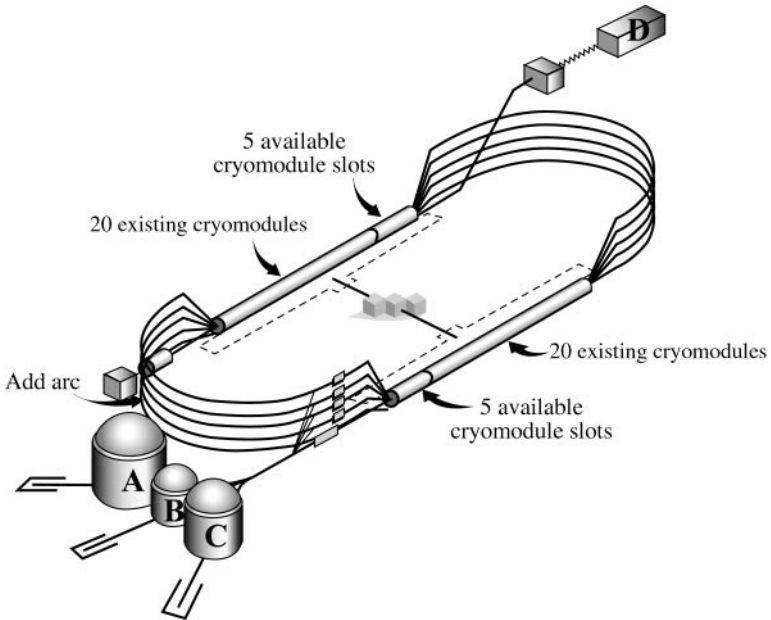


**Figure 12** Overview of the 12 GeV upgrade plan.

CEBAF's. Recent work (126), on the other hand, proceeds from the fact that the superconducting cavities developed for LEP and LEP-II will soon be available for other uses because of LHC installation. A seven-pass 25 GeV accelerator should be possible using the cavities that have already been built. At least two organizational hurdles must be overcome to make ELFE a reality. First, European nuclear physicists must be convinced that the ELFE project is sufficiently interesting to merit funding, and second, the cavities must be made available for this and not other projects.

**TABLE 2** Planned evolution of the CEBAF accelerator

	<b>6 GeV (present)</b>	<b>12 GeV (ca. 2004/5)</b>
Energy gain/pass	1.2 GeV	2.2 GeV
Number of passes	5	5.5
Cryomodules	Orig. @ 30 MV	Orig. + 10 new @ 100 MV
2 K cryoplant	4.8 kW	10 kW
Duty factor	cw	cw
Magnet system	Existing	Existing w/minor mods

## Energy-Recovered Linacs

As discussed above, CEBAF is operated at a beam current far below the ultimate limit for carrying current given by beam HOM heating and beam-breakup stability. Presently, the current is limited by the rf power installed on the site and by the beam power on the beam dump, which is already 1 MW at 5 GeV and 200  $\mu\text{A}$ . As mentioned, beam energy recovery is a way to overcome these limits; one can increase beam current without necessarily increasing the installed rf power or beam dump size. This basic idea was demonstrated at Stanford many years ago, and again recently in the Jefferson Lab IR Demo FEL at world-record average current (119).

Beam energy recovery is being vigorously developed for application in at least three new types of accelerators: electron-ion colliding beam machines, recirculating linac light sources driven by energy-recovered linacs (ERL), and high-average-power FELs. Present ideas call for increasing the beam average current to 100 mA or more, while still retaining a beam loss under 1  $\mu\text{A}$ , the limit for beam loss in the present CEBAF accelerator due to machine protection issues. The major new challenges common to all these proposals are

- producing a high-average-current gun with good beam quality, the proposals generally having beam current at least an order of magnitude beyond present experience,
- controlling the beam loss at the  $10^{-5}$  level, at least 20 times lower than present experience, and
- understanding the beam-cavity interactions and beam stability in these more highly loaded cases.

Less important for fundamental accelerator physics reasons, but certainly important for reducing the overall cost of final machine designs, work continues unabated to increase the gradient limits in the srf cavities to 25 MV/m and beyond.

Given that currents of order 100 mA or higher can be accelerated and energy-recovered properly, interesting applications are possible. An example recently discussed, relevant to the nuclear and particle physics community, is the Electron Ion Collider (EIC). In one rendering of this idea (127), an energy-recovered linac provides electrons for high-energy nuclear physics studies by colliding with a high-energy ion beam stored in a ring. At present, there seems to be no reason that such an energy-recovered linac could not be built with luminosities comparable to those that might be obtained with storage rings. There is good reason to believe, if a 1 A electron injector is possible, that a recirculating-linac-on-ring collider would have superior luminosity to ring-ring collider designs. The nuclear physics community is actively debating whether such colliders would have larger long-term impact than a fixed-target machine, such as a CEBAF further upgraded to 25 GeV.

Another application is to recirculating linac light sources. Because the emittance anticipated out of a 100 mA injector is small compared to the emittance of a storage ring synchrotron radiation source, and because the geometry of an

energy-recovered linac can support long straight regions that could support long undulators of length around 25 m, it is anticipated that an ERL light source can be built with X-ray brilliance superior to the present generation of synchrotron sources. Increases in average brilliance seem possible from around  $10^{19}$  at present to  $10^{22}$  photons/[sec mm<sup>2</sup> mrad<sup>2</sup> (0.1% bandwidth)] in an ERL light source.

As a final example, going to 100 mA beam current is the natural next upgrade step for the FEL work at Jefferson Lab, allowing of order 100 kW average power in the extracted laser beam. At such power levels, the FEL performance is more limited by the light optics than by any inherent limitation in the energy-recovered accelerator.

Scientists at Jefferson Lab are actively participating in such studies because knowledge developed at the laboratory during the CEBAF project has direct bearing on guiding the choices to be made for these newer projects.

## CONCLUSIONS

Jefferson Lab has built a unique accelerator that has met or exceeded all the goals set out in its original design. Many firsts and superlatives can be assigned to this accelerator: first application of srf technology over 100 active meters; world's first GeV-scale machine incorporating both beam recirculation and multiple interleaved beams; world's highest-average-current polarized electron source, routinely yielding over 10 C per day, with beam polarization above 75%; first demonstrations of the ability to produce and maintain short electron bunches on a routine basis in a production accelerator; world's highest-average-power cw electron beam; world's lowest extracted beam energy spread; and world's largest 2 K helium refrigeration system.

The accelerator now delivers beam to users reliably, with availability of order 70%. To achieve this availability, many systems had to be developed beyond the state-of-the-art at project inception. For example, the superconducting cavities themselves, as well as the physical processing done to the cavities during construction, evolved over time, eventually yielding accelerating gradients over twice the initial design value. In the initial stages of the project, the rf controls were so primitive that most of the cavities had to be hand-tuned in order to establish gradient in them, but now almost all cavity tuning is done automatically by the rf control hardware and software. The high-average-current polarized electron source was developed entirely during this project. Jefferson Lab was a leader in the establishment of the computer control system EPICS as a de facto standard for new large accelerators. Such developments are available to and can drive future planning of many interesting projects that have goals similar to those of the Jefferson Lab accelerator.

It is clear that through its ability to deliver high-average-power electron beams with superior beam quality, this accelerator proved that the formidable challenges to making srf technology useful and reliable on such a scale could be overcome. As a consequence, accelerator designers and physicists have a quite useful set of

new tools to apply in their future accelerator designs. In some applications, use of recirculating superconducting linacs makes possible previously unobtainable results. In the long term, perhaps this finding will be one of the most important results of the work on CEBAF at the Jefferson Laboratory.

## ACKNOWLEDGMENTS

The authors thank a number of generous colleagues for significant improvements to the manuscript. Isidoro Campisi, Lawrence Cardman, Claus Rode, and Charles Sinclair provided scientific and technical input, including text. Lia Merminga and Ronald Sundelin carefully read and commented on the manuscript. Jay Benesch and Thomas Hassler provided detailed technical performance information. Warren Funk contributed text on the Spallation Neutron Source. This work was supported by U.S. Department of Energy contract DE-AC05-84-ER40150.

**Visit the Annual Reviews home page at [www.AnnualReviews.org](http://www.AnnualReviews.org)**

## LITERATURE CITED

1. DOE/NSF Nuclear Science Advisory Committee. *Report of the NSAC ad hoc subcommittee on a 4 GeV cw electron accelerator for nuclear physics*. (Sept. 27, 1984)
2. Westfall C. *The founding of CEBAF, 1979 to 1987*. Hist. rep., Jefferson Lab archive (September 1994)
3. Banford PA. *Int. Adv. Cryogen. Eng.* 10:80 (1965)
4. Schwettman HA, Wilson PB, Pierce JM, Fairbank WM. *Int. Adv. Cryogen. Eng.* 10:88 (1965)
5. Sundelin R. *Proc. Third Workshop on RF Superconductivity* (ANL-PHY-88-1), ed. KW Shepard, p. 109. Chicago: Argonne Natl. Lab. (January 1988)
6. Furuya T, et al. *Proc. Third Workshop on RF Superconductivity* (ANL-PHY-88-1), ed. KW Shepard, p. 95. Chicago: Argonne Natl. Lab. (January 1988)
7. Sundelin RM. *IEEE Trans. Nucl. Sci.* NS-32:3570 (1985)
8. Westfall C. *The prehistory of Jefferson Lab's SRF accelerating cavities, 1962 to 1985*. Hist. rep., Jefferson Lab archive (April 1997)
9. Grunder HA, et al. *Proc. 1987 Part. Accel. Conf.*, p. 13
10. Grunder HA. *Proc. 1988 Linear Accel. Conf.*, p. 3
11. Leemann CW. JLab PR88-001 (1988)
12. Hartline BK. JLab PR 88-014 (1988)
13. Grunder HA. JLab PR 89-030 (1989)
14. Westfall C. *Jefferson Lab's 1985 switch to superconducting accelerator technology*. Hist. rep., Jefferson Lab archive (n.d.)
15. York RC, McCarthy JS, Norum BE. *IEEE Trans. Nucl. Sci.* 47:3259 (1983)
16. *CEBAF Conceptual Design Report*, Newport News, Va., February 1986
17. Rode CH, Proch D. *Proc. 1989 Part. Accel. Conf.*, p. 589
18. Douglas DR. *Proc. 1993 Part. Accel. Conf.*, p. 584
19. Douglas DR. JLab TN-97-038 (1997)
20. Douglas DR. JLab TN-98-008 (1998)
21. Poelker M. *Appl. Phys. Lett.* 67(19): 2762 (1995)
22. Hovater C, Poelker M. *Nucl. Instrum. Methods Phys. Res.* A418:280 (1998)
23. Lyneis CM, et al. *Proc. Conf. Future Possibilities for Electron Accelerators*, p. A1. Charlottesville: Univ. Va. (1979)

24. Bisognano JJ, Krafft GA. *Proc. 1986 Linear Accel. Conf.*, p. 452
25. Bisognano JJ, Gluckstern RL. *Proc. 1987 Part. Accel. Conf.*, p. 1078
26. Krafft GA, Bisognano JJ. *Proc. 1987 Part. Accel. Conf.*, p. 1356
27. Bisognano JJ. *Proc. Third Workshop on RF Superconductivity (ANL-PHY-88-1)*, ed. KW Shepard, p. 237. Chicago: Argonne Natl. Lab. (January 1988)
28. Bisognano JJ, Fripp ML. *Proc. 1988 Linear Accel. Conf.*, p. 388
29. Yunn BC. *Proc. 1991 Part. Accel. Conf.*, p. 1785
30. Sereno NS, et al. *Proc. 1993 Part. Accel. Conf.*, p. 3246
31. Campisi IE, Meringa L. JLab TN-98-011 (1998)
32. Campisi IE, et al. *Proc. 1993 Part. Accel. Conf.*, p. 1220
33. Mikijelj B, Campisi IE. *Proc. First Workshop on Microwave-Absorbing Materials for Accelerators (MAMAs)*, ed. IE Campisi, L Doolittle, p. 133. Newport News, Va.: Jefferson Lab (n.d.)
34. Ziman JM. *Electrons and Phonons; the Theory of Transport Phenomena in Solids*, pp. 334 ff. and 421 ff. Oxford, UK: Clarendon (1960)
35. Collin RE. *Field Theory of Guided Waves*, pp. 749 ff. New York: IEEE Press. 851 pp. 2nd ed. (1991)
36. Diamond WT. *Proc. 1987 Part. Accel. Conf.*, p. 1907
37. Diamond WT, Pico R. *Proc. 1988 Linear Accel. Conf.*, p. 403
38. Kneisel P, et al. *Proc. Conf. Electron Beam Melting and Refining State of the Art*, p. 177 (1990)
- 38a. Rao MG. *J. Vac. Sci. Technol.* A11(4): 1598 (1993)
39. Benesch JF, Reece CE. *Adv. Cryogen. Eng.* 39A:597 (1994)
40. Schneider W, et al. *Adv. Cryogen. Eng.* 39A:589 (1994)
41. Heckman J, et al. *Adv. Cryogen. Eng.* 41A:655 (1996)
42. Brindza P, Rode C. *Proc. 1986 Linear Accel. Conf.*, p. 76
43. Chronis WC, et al. *Proc. 1989 Part. Accel. Conf.*, p. 592
44. Rode CH. *Proc. 1989 Part. Accel. Conf.*, p. 589
45. Kashy D, Chronis WC, Rode C, Wilson J. *Adv. Cryogen. Eng.* 37A:577 (1992)
46. Rode CH. *Proc. 1995 Part. Accel. Conf.*, p. 1994
47. Krafft GA, Bisognano JJ, Miller R. JLab TN-87-50 (1987)
48. Fugitt JA, Moore TL. *Proc. 1986 Linear Accel. Conf.*, p. 70
49. Fugitt JA, Moore TL. *Proc. 1987 Part. Accel. Conf.*, p. 579
50. Hovater C, Fugitt J. *Proc. 1988 Linear Accel. Conf.*, p. 412
51. Simrock S, Hovater C, Jones S, Fugitt J. *Proc. 1989 Part. Accel. Conf.*, p. 1885
52. Simrock SN, et al. *Proc. 1990 Linear Accel. Conf.*, p. 480
53. Simrock S. *Proc. 1991 Part. Accel. Conf.*, p. 2515
54. Doolittle LR. *Proc. 1999 Part. Accel. Conf.*, p. 768
55. Krycuk A, Fugitt J, Mahoney K, Simrock S. *Proc. 1991 Part. Accel. Conf.*, p. 1470
56. Abbot R, et al. 1992 *Linear Accel. Conf. Proc.*, p. 232
57. Simrock SN, et al. *Proc. Second Eur. Part. Accel. Conf.*, p. 824 (1990)
58. Ashkenazi I, Lahti GE. *Proc. 1989 Part. Accel. Conf.*, p. 1861
59. Ursic R, Flood R, Piller C, Strong E. *Proc. 1997 Part. Accel. Conf.*, p. 2131
60. Hofler AS, et al. *Proc. 1993 Part. Accel. Conf.*, p. 2298
61. Powers T, Doolittle L, Ursic R, Wagner T. *Proc. Seventh Beam Instrum. Workshop, AIP Conf. Proc.* 390, p. 257 (1996)
62. Ursic R, et al. *Proc. Seventh Beam Instrumentation Workshop, AIP Conf. Proc.* 390, p. 405 (1996)
63. Douglas DR. *Proc. 1986 Linear Accel. Conf.*, p. 449

64. York RC, Douglas DR. *Proc. 1987 Part. Accel. Conf.*, p. 1292
65. Douglas DR, York RC, Kewisch J. *Proc. 1989 Part. Accel. Conf.*, p. 557
66. Bowling B, et al. *Proc. 1991 Part. Accel. Conf.*, p. 446
67. Douglas DR, York RC. *Proc. 1987 Part. Accel. Conf.*, p. 1295
68. York RC, Reece C. *Proc. 1987 Part. Accel. Conf.*, p. 1307
69. Barry A, Bowling B, Kewisch J, Tang J. *Proc. 1990 Linear Acc. Conf.*, p. 444
70. Douglas DR, Tang JY, York RC. *Proc. 1991 Part. Accel. Conf.*, p. 443
71. Douglas DR. *Proc. 1991 Part. Accel. Conf.*, p. 449
72. Bickley MH, Douglas DR, Servranckx RV. *Proc. 1991 Part. Accel. Conf.*, p. 309
73. van Zeijts J. *Proc. 1995 Part. Accel. Conf.*, p. 2356
74. Piot P, Krafft GA. *Proc. Sixth Eur. Part. Accel. Conf.*, p. 1327 (1998)
75. Li Z. *Beam dynamics in the CEBAF superconducting cavities*. PhD. thesis. College of William and Mary, Williamsburg, Va. (1995)
76. Leemann C, Yao CG. *Proc. 1990 Linear Accel. Conf.*, p. 232
77. Kazimi R, et al. *Proc 1992 Linear Accel. Conf.*, p. 244
78. Krycuk A, et al. *Proc. 1993 Part. Accel. Conf.*, p. 939
79. Kazimi R, et al. *Proc. 1993 Part. Accel. Conf.*, p. 1109
80. Harwood LH, et al. *Proc. 1989 Part. Accel. Conf.*, p. 399
81. Harwood L, Karn J. *Proc. Int. Conf. Magnet Technol., Victoria, Br. Columbia, Can.*, p. 2324 (1993)
82. Curtis C, Oren W, Tremblay KJ. *Proc. Third Int. Workshop on Accel. Alignment*, p. 9 (1993)
83. Bork R. *Proc. 1987 Part. Accel. Conf.*, p. 523
84. Watson WA III. *Proc. 1995 Part. Accel. Conf.*, p. 2167
85. Bickley M, White K. *Proc. 1995 Part. Accel. Conf.*, p. 2220
86. White KS, Bickley M, Watson W. *Proc. 1999 Int. Conf. on Accel. and Large Exp. Phys. Control Systems*, p. 17 (1999)
87. Tiefenback MG, Doolittle L, Benesch JF. *Proc. 1997 Part. Accel. Conf.*, p. 3758
88. Watson WA III. *Proc. 1997 Part. Accel. Conf.*, p. 2398
89. Bickley M, Bryan DA, White KS. *Proc. 1999 Part. Accel. Conf.*, p. 735
90. Bickley M, Chen J, Larrieu C. *Proc. 1999 Part. Accel. Conf.*, p. 741
91. Simrock S. *Proc. 1991 Part. Accel. Conf.*, p. 2515
92. Sinclair C. *Proc. 1992 Linear Accel. Conf.*, p. 3
93. Hutton A. *Proc. 1993 Part. Accel. Conf.*, p. 527
94. Merminga L, et al. *Proc. 1993 Part. Accel. Conf.*, p. 3515
95. Chao Y, et al. *Proc. 1993 Part. Accel. Conf.*, p. 587
96. Krafft GA. *Proc. 1994 Int. Linear Accel. Conf.*, p. 9
97. Grunder H. *Proc. 1995 Part. Accel. Conf.*, p. 1
98. Dunham BM. *Proc. XVIII Int. Linear Accel. Conf.*, p. 17 (1996)
99. Legg R. *Proc. Fifth Eur. Part. Accel. Conf.*, p. 130 (1996)
100. Reece CE, Drury M, Rao MG, Nguyen-Tuong V. *Proc. 1997 Part. Accel. Conf.*, p. 3105
101. Hutton A. *Proc. 1997 Part. Accel. Conf.*, p. 281
102. Krafft GA et al. *Proc. XX Int. Linear Accel. Conf.*, p. 721 (2000)
103. Sinclair CK. *Proc. 1999 Part. Accel. Conf.*, p. 65
104. Dunham B. *Investigations of the physical properties of photoemission polarized electron sources for accelerator applications*. PhD. thesis. Univ. Ill., Urbana-Champaign (1993)
105. Engwall D, et al. *Nucl. Instrum. Methods A* 324:409 (1993)
106. Steigerwald M. Presented at Polarized Electron Source Workshop, Nagoya, Jpn., Oct. 2000

107. Sinclair CK. JLab TN-96-032 (1996)
108. Jones M, et al. *Phys. Rev. Lett.* 84:1398 (2000)
109. Aniol KA, et al. *Phys. Rev. Lett.* 82:1096 (1999)
110. Alexa LC, et al. *Phys. Rev. Lett.* 82:1374 (2000)
111. Beise EJ, et al. *Phys. Rev. Lett.* 82:1379 (1999)
112. Beise EJ, et al. *Eur. Phys. J.* A7:421 (2000)
113. Krafft GA, Bisognano JJ. *Proc. 1989 Part. Accel. Conf.*, p. 1256
114. Neil G, Bisognano J, Dylla H, Krafft G. *Proc. 1991 Part. Accel. Conf.*, p. 2745
115. Bisognano JJ, et al. *Nucl. Instrum. Methods A* 318:216 (1992)
116. Neil GR, et al. *Nucl. Instrum. Methods A* 318:212 (1992)
117. Douglas DR, et al. JLab TN-91-071 (1991)
118. Benson SV. JLab ACT-96-05
119. Neil GR, et al. *Phys. Rev. Lett.* 84:662 (2000)
120. Piot P, Douglas DR, Krafft GA. *Proc. 2000 Eur. Accel. Conf.*, p. 1543 (2000)
121. Douglas DR. *Proc. 2000 Linear Accel. Conf.*, p. 716
122. Shinn M, et al. *Proc. SPIE* 3902:355 (2000)
123. Douglas DR, et al. *Proc. XX Int. Linear Accel. Conf.*, p. 857 (2000)
124. *The science driving the 12 GeV upgrade of CEBAF.* Jefferson Lab, Newport News, Va. (2001)
125. Bullard D, et al. *Proc. 1999 Part. Accel. Conf.*, p. 3309
126. Keil E. *Proc. 2000 Eur. Part. Accel. Conf.*, p. 33
127. Merminga L, Krafft GA, Lebedev V. Presented at EPIC Workshop, 2nd, MIT, Cambridge, Mass., Sept. 2000, and Int. Conf. High Energy Accel., 18th, Tsukuba, Jpn., March 2001